

Dispersive contour-path finite-difference time-domain algorithm for modelling surface plasmon polaritons at flat interfaces

Ahmad Mohammadi^{1,2}, and Mario Agio¹

¹*Nano-Optics Group, Laboratory of Physical Chemistry, ETH Zurich, CH-8093, Switzerland*

²*Department of Physics, Shiraz University, 71454 Shiraz, Iran*

Present address: Department of Physics, Persian Gulf University, 75169 Bushehr, Iran

mario.agio@phys.chem.ethz.ch

<http://www.nano-optics.ethz.ch>

Abstract: We investigate the accuracy of the two-dimensional Finite-Difference Time-Domain (FDTD) method in modelling Surface Plasmon Polaritons (SPPs) in the case of a single metal-dielectric interface and of a thin metal film showing that FDTD has difficulties in the low-group-velocity region of the SPP. We combine a contour-path approach with Z transform to handle both the electromagnetic boundary conditions at the interface and the negative dispersive dielectric function of the metal. The relative error is thus significantly reduced.

© 2006 Optical Society of America

OCIS codes: (240.6680) Surface plasmons; (000.4430) Numerical approximation and analysis; (130.0130) Integrated optics; (999.9999) FDTD methods

References and links

1. H. Raether, *Surface Plasmons on Smooth and Rough Surfaces and on Gratings* (Springer-Verlag, 1988)
2. W.L. Barnes, A. Dereux, and T.W. Ebbesen, "Surface plasmon subwavelength optics," *Nature* **424**, 824–830 (2003).
3. A. Taflove, and S.C. Hagness, *Computational Electrodynamics: The Finite-Difference Time-Domain Method* (Artech House, Norwood, MA, 2005).
4. D. Sullivan, *Electromagnetic Simulation Using the FDTD Method* (IEEE Press, 2000).
5. T.G. Jurgens, A. Taflove, K. Umaschankar, and T.G. Moore, "Finite-Difference Time-Domain Modeling of Curved Surfaces," *IEEE Trans. Antennas Propag.* **40**, 357–365 (1992).
6. C. Oubre, and P. Nordlander, "Optical Properties of Metalodielectric Nanostructures Calculated Using the Finite Difference Time Domain Method," *J. Phys. Chem. B* **108**, 17740–17747 (2004).
7. H. Shin, and S. Fan, "All-Angle Negative Refraction for Surface Plasmon Waves Using a Metal-Dielectric-Metal Structure," *Phys. Rev. Lett.* **96**, 073907(4) (2006).
8. K.-P. Hwang, and A.C. Cangellaris, "Effective Permittivities for Second-Order Accurate FDTD Equations at Dielectric Interfaces," *IEEE Microwave Wirel. Compon. Lett.* **11**, 158–160 (2001).
9. A. Mohammadi, and M. Agio, "Contour-path effective permittivities for the two-dimensional finite-difference time-domain method," *Opt. Express* **13**, 10367–10381 (2005), <http://www.opticsinfobase.org/abstract.cfm?URI=oe-13-25-10367>, and references therein.
10. M.K. Kärkkäinen, Subcell FDTD Modeling of Electrically Thin Dispersive Layers," *IEEE Trans. Microwave Theory Tech.* **51**, 1774–1780 (2003).
11. D. Popovic, and M. Okoniewski, "Effective Permittivity at the Interface of Dispersive Dielectrics in FDTD," *IEEE Microwave Wirel. Compon. Lett.* **13**, 265–267 (2003).

12. M. Born and E. Wolf, *Principles of Optics* (Cambridge U. Press, Cambridge, UK, 1999), 7th ed.
13. C.T. Chan, Q.L. Yu, and K.M. Ho, "Order- N spectral method for electromagnetic waves," *Phys. Rev. B* **51**, 16635–16642 (1995).
14. O. Ramadan, and A.Y. Oztoprak, "Z-transform implementation of the perfectly matched layer for truncating FDTD domains," *IEEE Microwave Wirel. Compon. Lett.* **13**, 402–404 (2003).
15. C. Kittel, *Introduction to Solid State Physics* (Wiley, New York, 1996), 7th ed.
16. In the error calculation we choose wavevectors $k \geq 1.5k_s$ (Fig. 3 and Fig. 4) and $k \geq 2.5k_s$ (Fig. 6) to focus on the low-group-velocity region.
17. The fit is performed using the logarithm of the error, so that the exponent α is obtained from $\log y = \alpha \log x + \log a$. The errors for $\Delta = 2 - 4\text{nm}$ are excluded from the fit since the Fourier error is of the same order of magnitude and thus it may have an effect on the actual FDTD accuracy.
18. C. Hulse, and A. Knoesen, "Dispersive models for the finite-difference time-domain method: design, analysis, and implementation," *J. Opt. Soc. Am. A* **11**, 1802–1811 (1994).

1. Introduction

The optical properties of metallic nanostructures supporting Surface Plasmon Polaritons (SPPs) are very interesting for a wide range of applications operating at near-infrared and visible wavelengths [1, 2]. Nanofabrication techniques and quantitative modelling tools are key requirements for the realization of novel devices. In this context, the Finite-Difference Time-Domain (FDTD) method [3, 4] has become very popular thanks to its flexibility in handling arbitrary shapes with a simple and robust algorithm. While FDTD has been significantly improved for the treatment of metals at microwave frequencies [3, 5], its applications in the near-infrared and visible range is still challenging, especially for the treatment of SPPs at the metal-dielectric interface. A brute force solution to this problem is using extremely fine meshes [6, 7], with the consequence that high-level computing resources become necessary.

In fact, both for dielectrics and perfect conductors it has been pointed out that the enforcement of the electromagnetic boundary conditions improves the convergence of the algorithm [5, 8, 9]. Recent works have applied similar ideas to the modelling of dispersive materials [10, 11]. The peculiarity of SPPs though, is that the electromagnetic field is TM polarised, with a parallel and orthogonal electric field components strongly localised at the interface. For these reasons, SPPs will be even more sensitive to the way interfaces are implemented in FDTD. Figure 1 sketches a two-dimensional (2D) FDTD mesh around a flat metal-dielectric interface. In the FDTD algorithm, when a cell is partially filled it is replaced by a homogeneous cell with the material that occupies more than half of it, hence the so-called *staircase* approximation. Moreover, the field components must be displaced in space and time to construct the finite-difference equations [3]. For these reasons, the longitudinal and transverse electric components of a SPP will sense different interfaces. Therefore, regardless of the position, FDTD is unable to fit the correct conditions of a SPP even for a flat interface.

In this work we extend the 2D Contour-Path (CP) FDTD algorithm [5, 9] to interfaces aligned with the mesh for dispersive materials and discuss the effects of staircasing on SPPs by considering a metal-dielectric interface and a thin metal film. We show that by this approach, which rigorously enforces the electromagnetic boundary conditions, a significant improvement in the modelling of SPPs is achieved.

2. Dispersive contour-path method

We consider two semi-infinite isotropic and non-magnetic media forming a flat interface, with dielectric functions ϵ_d and $\epsilon_m(\omega) = \epsilon_\infty - \omega_p^2 / (\omega(\omega + i\gamma))$, respectively; ω_p is the plasma frequency and γ is the damping frequency [12]. The constitutive relations $\mathbf{B} = \mathbf{H}$ and $\mathbf{D} = \epsilon_m(\omega)\mathbf{E}$, where μ_0 and ϵ_0 are set to 1, must be expressed in time domain to be compatible with the FDTD paradigm. Therefore, the relationship between \mathbf{D} and \mathbf{E} becomes a convolution. We use the Z transform as a suitable transformation to replace discrete convolutions with multiplications [4],

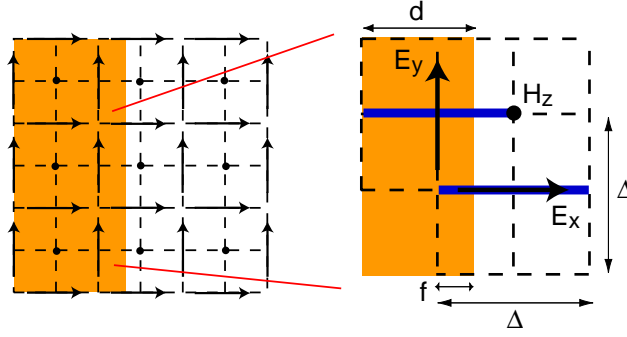


Fig. 1. Layout of the FDTD mesh on the metal-dielectric interface (metal at the left). The integration paths for E_y and E_x are marked by thick lines.

so that the constitutive relation for \mathbf{D} and \mathbf{E} becomes for each field component

$$D(z) = \epsilon_m(z)E(z)\Delta t, \quad (1)$$

where Δt is the time step used in FDTD and $\epsilon_m(z)$ corresponds to $\epsilon_m(\omega)$ in z -space

$$\epsilon_m(z) = \frac{\epsilon_\infty}{\Delta t} + \frac{\omega_p^2}{\gamma} \left(\frac{1}{1-z^{-1}} - \frac{1}{1-z^{-1}e^{-\gamma\Delta t}} \right). \quad (2)$$

Equation (1) can be rearranged as follows with the help of an auxiliary term $S(z)$

$$E(z) = D_a D(z) - z^{-1}S(z), \quad (3)$$

$$S(z) = C_a z^{-1}S(z) - C_b z^{-2}S(z) + C_c E(z), \quad (4)$$

with coefficients

$$\begin{aligned} C_a &= 1 + e^{-\gamma\Delta t}, & C_b &= e^{-\gamma\Delta t}, \\ C_c &= \frac{\omega_p^2 \Delta t}{\gamma \epsilon_\infty} (1 - e^{-\gamma\Delta t}), & D_a &= \frac{1}{\epsilon_\infty}. \end{aligned} \quad (5)$$

A detailed derivation of Eqs. (1-4) can be found in Ref. [4]. Notice that the form of Eq. (4) and its coefficients are determined by $\epsilon_m(\omega)$, i.e. by the dispersion model. Since in the Z space, z^{-1} works as a delay operator [4], the implementation of these equations in FDTD is straightforward and reads

$$\begin{aligned} E|^{n+1} &= D_a D|^{n+1} - S|^{n+1}, \\ S|^{n+1} &= C_a S|^{n+1} - C_b S|^{n+1} + C_c E|^{n+1}, \end{aligned} \quad (6)$$

where $|^{n+1}$ represents the field at time $t = (n+1)\Delta t$.

To properly account for the electromagnetic boundary conditions, we derive the FDTD algorithm starting from the Maxwell's equations in integral form [3, 9]. As depicted in Fig. 1, because we are dealing with a flat interface, we refer to a 2D mesh with TM polarised light (non-zero field components E_x , E_y , H_z). Consider first the E_y component, which is parallel to the interface. The FDTD integration path associated to Ampère law is partially inside the metal and partially in the dielectric. For this reason, we introduce an average dielectric displacement

$$D = \frac{d}{\Delta} D_m + \left(1 - \frac{d}{\Delta}\right) D_d, \quad (7)$$

where d and Δ are defined in Fig. 1, D_m and D_d refer to the electric displacement in metal and dielectric, respectively, and the y subscript is omitted. Using Eq. (3) and exploiting the boundary condition $E_m = E_d \equiv E$, we obtain

$$D(z) = \varepsilon_{\parallel} E(z) + \frac{d}{\Delta} \varepsilon_{\infty} z^{-1} S_m(z), \quad (8)$$

where $\varepsilon_{\parallel} = \frac{d}{\Delta} \varepsilon_{\infty} + \left(1 - \frac{d}{\Delta}\right) \varepsilon_d$ [8, 9]. Therefore, by saving D and $S \equiv \frac{d}{\Delta} \frac{\varepsilon_{\infty}}{\varepsilon_{\parallel}} S_m$ in memory, we can keep the same formulae as Eq. (6) and change the coefficients of Eq. (5) as follows

$$C_c = \frac{d}{\Delta} \frac{\omega_p^2 \Delta t}{\gamma \varepsilon_{\parallel}} (1 - e^{-\gamma \Delta t}), \quad D_a = \frac{1}{\varepsilon_{\parallel}}. \quad (9)$$

Now consider the E_x field component, which is perpendicular to the interface. The integration path of Faraday law is again partially inside the metal and partially in the dielectric, as shown in Fig. 1. Following the same idea, we introduce an average electric field

$$E = \frac{f}{\Delta} E_m + \left(1 - \frac{f}{\Delta}\right) E_d, \quad (10)$$

where f is defined in Fig. 1 and the x subscript is omitted. Using Eq. (3) and the boundary condition $D_m = D_d \equiv D$, we obtain

$$E(z) = \frac{D(z)}{\varepsilon_{\perp}} - \frac{f}{\Delta} z^{-1} S_m(z), \quad (11)$$

where $\varepsilon_{\perp} = \left[\frac{f}{\Delta} \frac{1}{\varepsilon_{\infty}} + \left(1 - \frac{f}{\Delta}\right) \frac{1}{\varepsilon_d} \right]^{-1}$ [8, 9]. To update $S_m(z)$, the electric field inside the metal is needed, which can be obtained from E . After a few simple algebraic operations and by saving E and $S \equiv \frac{f}{\Delta} S_m$ in memory, we can use the same formulae as Eq. (6) and change the coefficients of Eq. (5) as follows

$$\begin{aligned} C_a &= 1 + e^{-\gamma \Delta t} - \left(1 - \frac{f}{\Delta} \frac{\varepsilon_{\perp}}{\varepsilon_{\infty}}\right) \frac{\omega_p^2 \Delta t}{\gamma \varepsilon_{\infty}} (1 - e^{-\gamma \Delta t}), \\ C_c &= \frac{\varepsilon_{\perp}}{\varepsilon_{\infty}} \frac{f}{\Delta} \frac{\omega_p^2 \Delta t}{\gamma \varepsilon_{\infty}} (1 - e^{-\gamma \Delta t}), \quad D_a = \frac{1}{\varepsilon_{\perp}}. \end{aligned} \quad (12)$$

3. Numerical tests and discussion

In order to compare the accuracy of the CP method with respect to staircasing and investigate how well FDTD can model SPPs, we use the 2D-FDTD method to compute the dispersion relation $\omega(k)$ of SPPs propagating along a single metal-dielectric interface and along a thin metal film. These systems are chosen for two reasons; first because they have an analytical solution, which we can take as reference [1]; second because they represent the simplest cases for understanding the basic issues of FDTD in handling SPPs.

3.1. Single metal-dielectric interface

For a metal-dielectric interface, the dispersion relation $\omega(k)$ of SPPs is given by [1]

$$k = \frac{\omega}{c} \left[\frac{\varepsilon_d \varepsilon_m(\omega)}{\varepsilon_d + \varepsilon_m(\omega)} \right]^{1/2}. \quad (13)$$

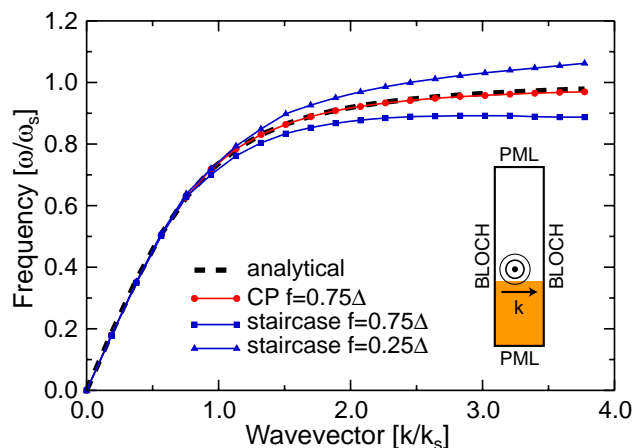


Fig. 2. Dispersion relation for a SPP at a glass/copper interface. Frequencies and wavevectors are expressed in units of $\omega_s = \omega_p / (\epsilon_d + \epsilon_\infty)^{1/2}$ and $k_s = \omega_s \sqrt{\epsilon_d} / c$ ($\lambda_s = 2\pi/k_s \simeq 450\text{nm}$). The discretization corresponds to $\Delta = 5\text{nm}$. Inset: simulation scheme, see text for details.

The calculation scheme is shown in the inset to Fig. 2. The FDTD mesh has Bloch boundary conditions [13] at the terminations perpendicular to the interface and PML [14] boundary conditions at the remaining sides. A dipole placed in the proximity of the interface excites the SPP. Because of the Bloch boundary conditions, only the energies corresponding to the imposed wavevector survive as time evolves. By Fourier transforming the recorded time series, one obtains frequency peaks, which yield the SPP dispersion relation when considering all wavevectors [13].

As an example of metal-dielectric interface we choose glass ($\epsilon_d = 2.25$) and copper ($\epsilon_\infty = 1.0$, $\omega_p = 5.0 \times 10^{15}\text{rad/s}$ and $\gamma = 0.01\omega_p$) [15]. The dispersion relations computed using staircasing, the CP method and the analytical solutions are plotted in Fig. 2. While in the region where the SPP has a high group velocity both methods agree very well with the analytical curve, as the group velocity decreases staircasing exhibits a much larger error. Indeed, this is the case where the SPP is tightly localised at the interface and thus a proper treatment of the electromagnetic boundary conditions is more important. In fact, the relative error $|\omega(k)_{\text{FDTD}} - \omega(k)|/\omega(k)$ increases linearly with k for frequencies in the flat region of the dispersion relation ($k \geq k_s$), for both staircase and CP.

To investigate the behaviour of staircasing and our CP method further, we compute the dispersion relation for different discretizations Δ . Figure 3 plots the average relative error $\frac{1}{N} \sum_k |\omega(k)_{\text{FDTD}} - \omega(k)|/\omega(k)$, where N is the number of wavevectors used in the sum [16] and $\omega(k)$ is the solution to Eq. (13). While the CP error remains small for a wide range of cell sizes, the staircasing one grows rapidly and becomes larger than 10% already for discretizations as small as $\Delta = 10\text{nm}$. By fitting the curves of Fig. 3 with the function $y = a\Delta^\alpha$ we can estimate the order of convergence [17]. While staircasing is only first-order accurate ($\alpha = 0.95 \pm 0.02$), the CP-FDTD exhibits $\alpha = 1.47 \pm 0.1$. We have found basically the same values for α by fitting the L^2 error $\frac{1}{N} [\sum_k |\omega(k)_{\text{FDTD}} - \omega(k)|^2 / \omega(k)^2]^{1/2}$. Notice that even if our CP approach fulfils the boundary conditions at the interface, it does not gain second-order accuracy ($\alpha = 2$) as it occurs for interfaces between dielectric materials [8] and in a homogeneous medium [3].

To gain more insight on this point, since we are essentially computing a dispersion relation on an FDTD grid, we give an analytical expression for it following the same method described

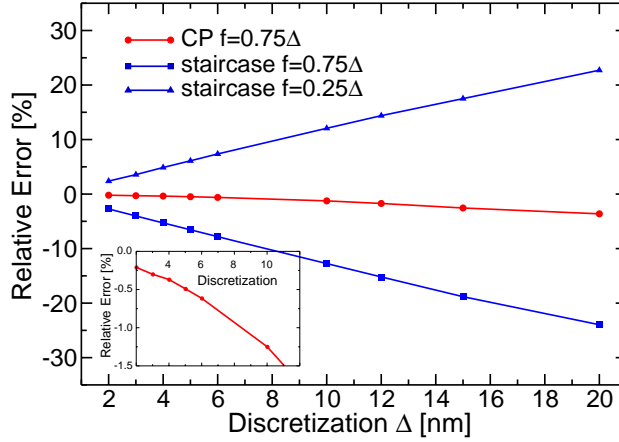


Fig. 3. Relative error as a function of discretization Δ . Only discretizations that divide the mesh along k are considered in order to keep its length constant. The frequency relative error in the Fourier transform is kept below 0.2%. Inset: zoomed error for the CP method. We can assign a positive or negative sign to the error because the FDTD result is always above or below the exact one, as shown in Fig. 2.

in Ref. [3] for a plane wave in a homogeneous medium. Assuming $\gamma = 0$, as trial solution we take the following SPP mode

$$\begin{aligned}
 E_x|_{i,j+1/2}^{n+1} &= E_{x,0} \exp\{i[k_i\Delta - \tilde{\omega}(n+1)\Delta t] - \tilde{k}(j+1/2)\Delta\}, \\
 E_y|_{i+1/2,j}^{n+1} &= E_{y,0} \exp\{i[k(i+1/2)\Delta - \tilde{\omega}(n+1)\Delta t] - \tilde{k}j\Delta\}, \\
 H_z|_{i,j}^{n+1/2} &= H_{z,0} \exp\{i[k_i\Delta - \tilde{\omega}(n+1/2)\Delta t] - \tilde{k}j\Delta\},
 \end{aligned} \quad (14)$$

where i, j point to an FDTD cell. Notice that k is exact since it is set by the Bloch boundary conditions, while the lateral confinement \tilde{k} and the frequency $\tilde{\omega}$ are affected by the discretization Δ . Moreover, \tilde{k} and $E_{x,0}$ are different in the dielectric and in the metal. After substituting Eqs. (14) into the Yee algorithm, eliminating the common exponential factors and applying the boundary conditions at the metal-dielectric interface, we obtain the expression for the SPP dispersion relation on the FDTD mesh,

$$\sin\left(\frac{k\Delta}{2}\right) = \frac{1}{S_c} \left[\frac{\epsilon_d \epsilon_m(\tilde{\omega})}{\epsilon_d + \epsilon_m(\tilde{\omega})} \right]^{1/2} \sin\left(\frac{\tilde{\omega}\Delta t}{2}\right), \quad (15)$$

where S_c is the Courant stability factor [3], which in our numerical experiments is 0.95. By computing the relative error for different discretizations Δ and fitting it with $y = a\Delta^\alpha$, as we have done for the data in Fig. 3, we obtain $\alpha = 2$, like for a homogeneous medium. In deriving Eq. (15) we assumed that the boundary conditions are fulfilled and that the dielectric function in the metal is exactly $\epsilon_m(\tilde{\omega})$ at $\tilde{\omega}$. Since material dispersion in FDTD enters through a convolution between $\epsilon_m(n\Delta t)$ and the electric field, which is also affected by the discretization, we expect also an error for $\epsilon(\tilde{\omega})$ at $\tilde{\omega}$. Following the guidelines of Ref. [18], it is easy to find that the Z transform applied to Drude dispersion implies an error proportional to $\omega_p^2 \Delta t^2$. Therefore, Eq. (15) should be corrected as

$$\sin\left(\frac{k\Delta}{2}\right) = \frac{1}{S_c} \left[\frac{\epsilon_d (\epsilon_m(\tilde{\omega}) + \omega_p^2 \Delta t^2 / 4)}{\epsilon_d + \epsilon_m(\tilde{\omega}) + \omega_p^2 \Delta t^2 / 4} \right]^{1/2} \sin\left(\frac{\tilde{\omega}\Delta t}{2}\right). \quad (16)$$

Once again we compute the relative error for Eq. (16) and fit it to the curve $y = a\Delta^\alpha$ to estimate the order of convergence. We find that α remains equal to 2, which makes sense given that the error on $\varepsilon(\omega)$ is second-order in Δt . The fact that α does not reach 2 for the CP method should therefore be attributed to other sources of error. We very much believe that the major problem resides in the Bloch boundary conditions, which are not fully correct for a system with losses. Indeed, by testing our method on a system with significantly lower losses we obtained $\alpha \simeq 1.8$. We could not test a system without losses because FDTD must fulfil the causality condition for the dielectric function. Despite this problem we are confident that the relative improvement of the CP method against staircasing remains valid, because the boundary conditions affect both algorithms equally.

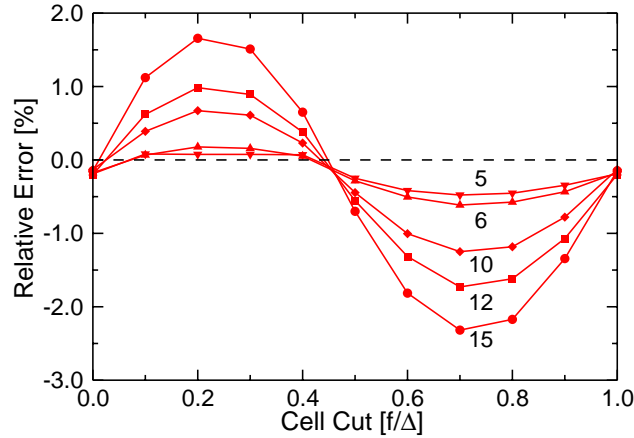


Fig. 4. Relative error for the CP method as a function of the cell cut f for various discretizations Δ . The label to each curve refers to Δ expressed in nm. $f/\Delta = 0.0$ is equivalent to $f/\Delta = 1.0$. We can assign a positive or negative sign to the error because the FDTD result is always above or below the exact one, as shown in Fig. 2.

Another relevant aspect is the dependence of the error on the position of the cell cuts d and f shown in Fig. 1. Actually, d and f are not independent, because $d = f + 0.5\Delta$ if $f < 0.5\Delta$ or $d = f - 0.5\Delta$ if $f \geq 0.5\Delta$. Therefore, it is enough to study the case when f varies from 0 to Δ . Notice that staircasing implies only two situations $f < 0.5\Delta$ and $f \geq 0.5\Delta$ that exhibit different errors as it can be inferred from Figs. 2 and 3. On the contrary, the CP method is able to account for the exact value of f . This property is very important for optimisation algorithms where a structure parameter is finely tuned. The result, plotted in Fig. 4, shows that the error depends on f in a non-trivial manner. The error is larger when f/Δ is about 0.75 and, like for staircasing, it is positive for $f/\Delta \simeq 0.25$ and negative for $f/\Delta \simeq 0.75$. The minimum error is found for $f/\Delta \simeq 0.5$, corresponding to the situation where the cell associated to the parallel field component is completely filled with metal, and for $f/\Delta \simeq 1.0$ or 0.0 , corresponding to the situation where the cell associated to the perpendicular field component is completely filled with metal. In other words, the best performances are obtained when the dispersive CP operates only on one field component. In this perspective, one could think of positioning the mesh so that only one CP integral is used, i.e. only one field component has a partially filled cell [11]. However, since the error remains small over the full range of f , we believe that avoiding such constraint would be more advantageous for modelling general structures.

3.2. Thin metal film with symmetric interfaces

We now consider a slightly more complex system made of a copper thin film (thickness $d = 50\text{nm}$) in glass. With respect to the previous case we have two new features: the interaction of SPPs bound at the two interfaces and the existence of a dimension for the structure i.e. the film thickness. The staircasing error therefore arises both from the individual interfaces and from the imperfect matching of the film thickness, which is responsible for the SPP coupling.

Since the structure is symmetric, the normal modes of the system are antisymmetric (ω_+) and symmetric (ω_-) SPPs. Their dispersion relations are given in implicit form by the following equations [1],

$$\begin{aligned}\omega_+ : \epsilon_m k_d + \epsilon_d k_m \tanh \frac{k_m d}{2l} &= 0, \\ \omega_- : \epsilon_m k_d + \epsilon_d k_m \coth \frac{k_m d}{2l} &= 0,\end{aligned}\quad (17)$$

where $k_{m,d} = \left(\epsilon_{m,d} \frac{\omega^2}{c^2} - k^2 \right)^{1/2}$. The computational scheme, shown in the inset to Fig. 5 is essentially equal to the previous test. A comparison between staircasing, CP and the analytical result is displayed in Fig. 5. Again, the CP method agrees very well with the analytical curve even in the low-group-velocity region, where staircasing becomes inaccurate. However, it seems that the situation is not as bad as for the single interface.

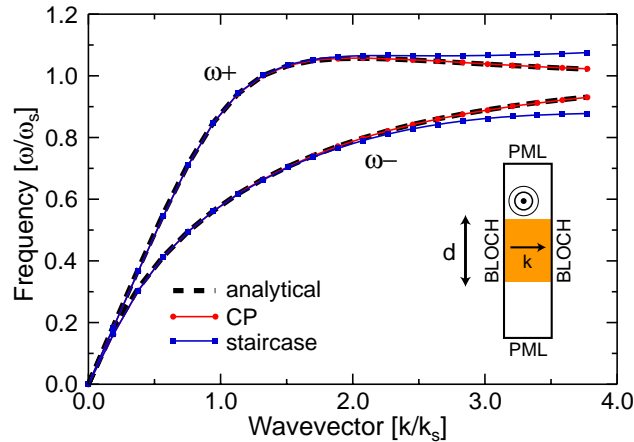


Fig. 5. Dispersion relation for symmetric (ω_-) and antisymmetric (ω_+) SPP at a glass/copper/glass thin film (thickness $d = 50\text{nm}$). Frequencies and wavevectors are expressed in the same units of Fig. 2. The discretization corresponds to $\Delta = 5\text{nm}$. Inset: simulation scheme, see text for details.

To clarify this point, we have calculated the relative error for different discretizations. Figure 6 reveals that the case of Fig. 5 is a special one. Indeed, $\Delta = 5\text{nm}$ matches exactly the film thickness; moreover, if the upper interface has $f = 0.75\Delta$, the lower one will have $f = 0.25\Delta$, and vice versa. Because we see from Fig. 2 that one curve is above and the other one is below the correct result, it could happen that their coupling into symmetric and antisymmetric modes luckily reduces the error, explaining the dip in Fig. 6. The same occurs for the CP method since it also exhibits the change of sign in the error as shown in Fig. 4. Notice that this effect occurs also for $\Delta = 2\text{nm}$, which shows up as a steeper drop in the error. It is not so evident for the

CP method though, because for such discretization we have already reached the error on the Fourier transform. These findings suggest that under certain conditions one could reduce the error more rapidly than at the rate set by α . On the other hand, such route seems not realistic for complicated structures, where the various cancelling effects cannot be guided by intuition. What is important here is that, again, the CP approach is always nearly an order of magnitude better than staircasing.

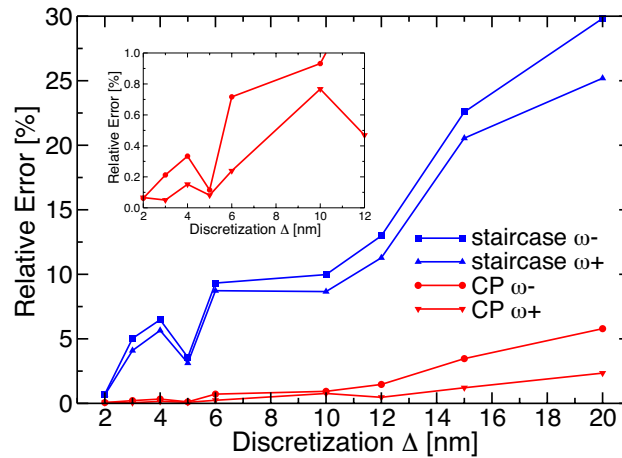


Fig. 6. Relative error as a function of discretization Δ . The frequency relative error in the Fourier transform is kept below 0.2%. Lower inset: zoomed error for the CP method.

4. Conclusions

In conclusion, we have demonstrated the difficulties of the FDTD algorithm in modelling SPPs even for the simplest cases of a single metal-dielectric interface and a thin metal film. The issue originates from the displacement of the field components in the FDTD mesh, the staircase approximation and the strong field localisation at the interface. We have proposed a CP-FDTD approach in combination with Z transform that is able to significantly reduce the relative error. Our method is readily extendable to three-dimensions, where two field components are parallel and the third one is perpendicular to the interface, if the latter is aligned with the mesh. In this case, the line integrals of Ampère law become surface integrals, but Eq. (9) remains valid. Moreover, our approach is in principle valid for any dispersion model.

The formulae derived in this work are applicable only to interfaces aligned with the mesh. We are aware that to fully improve FDTD one would need a similar way for treating tilted interfaces; we think that our Z-transform-based CP method could be a good starting point. The ability to reduce the error by an order of magnitude for general structures would indeed represent a significant advancement in modelling SPPs using FDTD.

Acknowledgements

We thank Vahid Sandoghdar for continuous support and encouragement. This work was financed by the ETH Zurich initiative on Composite Doped Metamaterials (CDM).